



## Structural Property Improvements of Bentonite with Sulfuric Acid Activation

Suna BALCI<sup>1\*</sup>

<sup>1</sup>Department of Chemical Engineering, Faculty of Engineering, Gazi University, 06570, Ankara, Turkey

**Abstract:** The acid activation of bentonite from Middle Anatolia, consisting of mostly montmorillonite, with a hot solution of H<sub>2</sub>SO<sub>4</sub> with different concentrations was carried out. SEM images, nitrogen sorption isotherms and FTIR spectra were used to examine the structural changes of the bentonite with acid activation. Acid-base titration method was applied to determine the surface acidities. The characterization results indicated that the acid activation caused considerable increases in the surface area and pore volumes by changing both the morphology and surface properties. The increase of the acid strength resulted in enhancement both in the surface area and acid sites up to 2 M concentration. For both Lewis and Brønsted acidities, significant increases occurred in addition to H-bonding to the structure.

**Keywords:** Bentonite, acid activation, leaching, textural properties, surface acidity.

**Submitted:** August 31, 2017. **Accepted:** April 24, 2018.

**Cite this:** Balci S. Structural Property Improvements of Bentonite with Sulfuric Acid Activation. JOTCSB. 2018;1(2):201-12.

**\*Corresponding author.** E-mail: [sunabalci@gazi.edu.tr](mailto:sunabalci@gazi.edu.tr).

## INTRODUCTION

Studies related to improving the surface properties of natural porous materials are always hot topics in terms of their economic viability. Clay minerals are used extensively as adsorbents and catalyst supports and their adsorption characteristics strongly depend on textural, structural, and morphological characteristics, in addition to their chemical composition and impurities. Smectites are characterized by a 2:1 layer structure in which two silica tetrahedral sheets form on either side of an aluminum octahedral sheet through sharing of apical oxygens and are one of the largest and most important classes of the phyllosilicate clay-mineral group (1-3). Bentonite is considered to be an impure clay that consists mainly of the smectite montmorillonite in terms of its mineralogy. Although their high cation exchange capacity and expanding layer properties, the absence of lasting high porosity and surface area are the main disadvantages of the smectite clays during the application. The modifications, which are performed before use, cause improvements in the structural and textural characteristics hence increase their application efficiency (1, 3-7). During such treatments, porosity, surface area, and number of active sites within the crystal matrix increase. Activation with a strong inorganic acid (partially preferred ones HCl and H<sub>2</sub>SO<sub>4</sub>), is the most commonly used pre-treatment technique (8-20). Although the properties of the end product depends on the characteristics of bentonite and its montmorillonite content, the activated material possess a high activation capacity and is suitable as adsorbent with an application of heavy metal removal (21) as a bleaching earth which has an application in food industry such as oil purification, decolorization of juice, etc. (10, 12, 22). Nowadays the studies searching the positive effects of acid activation on catalytic properties has gone up especially for organic synthesis (23-26).

Acid treatment of clays causes the replacement of the exchangeable cations with H<sup>+</sup> ions resulting increases in surface acidity and leaching of Al and other cations out of both octahedral and tetrahedral sheets to some degree resulting significant deterioration of SiO<sub>4</sub> groups (19). The most important physical changes in activated smectites by the removal of desired portion of the octahedral cations is the development of the new pores and the increase of the porosity leading to a considerable rise in the surface with the increased surface acidity. In addition to the increased bleaching capacity, the increase of filtration capacity, which depends on the quantity of larger size pores is also important in their applications. The good estimate by patents is the presence of around 15-20% macropores within the end product (27-30). Literature studies have shown that acid activation with hot mineral acid causes considerable increases in the adsorptive and catalytic power of the mineral under intermediate activation conditions. However, collapsing of the clay framework under severe activation conditions could be a problem. In the present study, changes in the surface properties of the bentonite from Turkey by acid activation using dilute sulfuric acid were studied by

scanning electron microscopy (SEM) images, nitrogen adsorption isotherms, acid-base titration, and Fourier transform infrared (FTIR) spectroscopy.

## MATERIALS AND METHODS

In this study, the natural bentonite from the Hancili region (Central Anatolia, Turkey), which is called Hancili White Bentonite (HWB), whose physicochemical and mineralogical characteristics were previously reported (31), was used. The mineralogical analysis showed that the bentonite was in type of montmorillonite (> 85%). The acid modification of the bentonite having particles of less than 200 mesh was performed using various concentrations of H<sub>2</sub>SO<sub>4</sub> ranging from 1.0 to 3.0 M for 4 hours at boiling point under reflux recycle to prevent loss of solution keeping the solid to solution ratio as 0.1 g clay cm<sup>-3</sup> under continuous stirring. Activated samples were separated by vacuum filtration, then washed several times by demineralized water until reaching near neutral filtrate water and no sulfate ions. The filtrate was dried at ±105°C for 3 h and subsequently ground.

The alteration in Al/Si ratio with acid treatment was investigated from the measurements of chemical composition by semi-quantitative EDS (Philips XL-30S FEG energy dispersive X-ray spectrometer) analysis, in a depth between 500 nm and 1000 nm. SEM photograph of the samples were taken by JEOL JSM-840A scanning electron microscope. The nitrogen sorption isotherms were obtained on a Quantachrome Autosorb 1C at 77 K. Prior to measurements, the oven dried samples for 12 h were degassed at 300 °C under high vacuum (10<sup>-6</sup> bar) for 3 hours and then the adsorption/desorption isotherms were taken. BET surface area ( $S_{BET}$ ) values were determined within  $P/P_0$  values of 0.05 – 0.30. The micro pore ( $V_{\mu}$ ), and micro+meso pore volume ( $V_{\mu+m}$ ) and total pore volume values were estimated from desorption data at  $P/P_0$  values of ~0.02, 0.96, and 0.99, respectively. The pore volume percentages were calculated over total pore volume. The variations of the surface functional groups were investigated by recording the FTIR spectra of the ~1 gram of samples with 100 grams of KBr pressed on disks which were taken on an ATI UNICAM MATTSON 100 in the range of 400 – 4000 cm<sup>-1</sup>. Surface acidities in terms of N eqv NaOH per 100 g of solid were determined by acid-base titration method by use of 1 M NaOH solution (32).

## RESULTS AND DISCUSSION

The physicochemical properties estimated from several characterization techniques are summarized in Table 1. The starting bentonite had an Al/Si ratio of 0.25 and by acid activation mainly in octahedral layer composition has changed to decreases in that ratio. This leaching might result from the formation of new pores within the clay sheets, although some leaching of silicon from tetrahedral sheets caused the distortion and opening of the clay layers creating increases in the mesopores.

**Table 1:** Physicochemical properties of raw bentonite and the acid activated ones.

<b>Property</b>	<b>Sample as-mined</b>	<b>activated with 1 M H<sub>2</sub>SO<sub>4</sub></b>	<b>activated with 2 M H<sub>2</sub>SO<sub>4</sub></b>	<b>activated with 3 M H<sub>2</sub>SO<sub>4</sub></b>
Al/Si	0.25	0.20	0.19	0.17
BET surface area, S <sub>BET</sub> (m <sup>2</sup> .g <sup>-1</sup> )	52.77	129.22	131.15	130.03
Micro pore volume, V <sub>μ</sub> (cm <sup>3</sup> .g <sup>-1</sup> )	0.0139	0.0232	0.0340	0.0325
Micro+meso pore volume, V <sub>μ+m</sub> (cm <sup>3</sup> .g <sup>-1</sup> )	0.1055	0.1758	0.2210	0.270
% micro pore volume	6.53	7.34	10.52	7.99
% meso pore volume	51.64	51.54	57.81	58.39
Surface acidity, N <sub>eqv</sub> /100 g	46	144	160	244

SEM micrographs of the crude bentonite and acid-activated samples are seen in Figure 1. The raw mineral exhibited a typical layered structure with a smooth surface and it was seen that the leafy appearance was altered by acid treatment resulting in tightly packed structure. The morphological deterioration became dominant with an increase of acid strength as the result of metal leaching both from the octahedral and tetrahedral sheets. This leaching firstly led to a formation of new pores. With the further increase of acid concentration the fracture of the particles and pore walls began crumbling, causing a decrease in particle size. This collapse of the pore wall could give a lead to the formation of bigger size pores by the formation of probably amorphous Si-rich material.

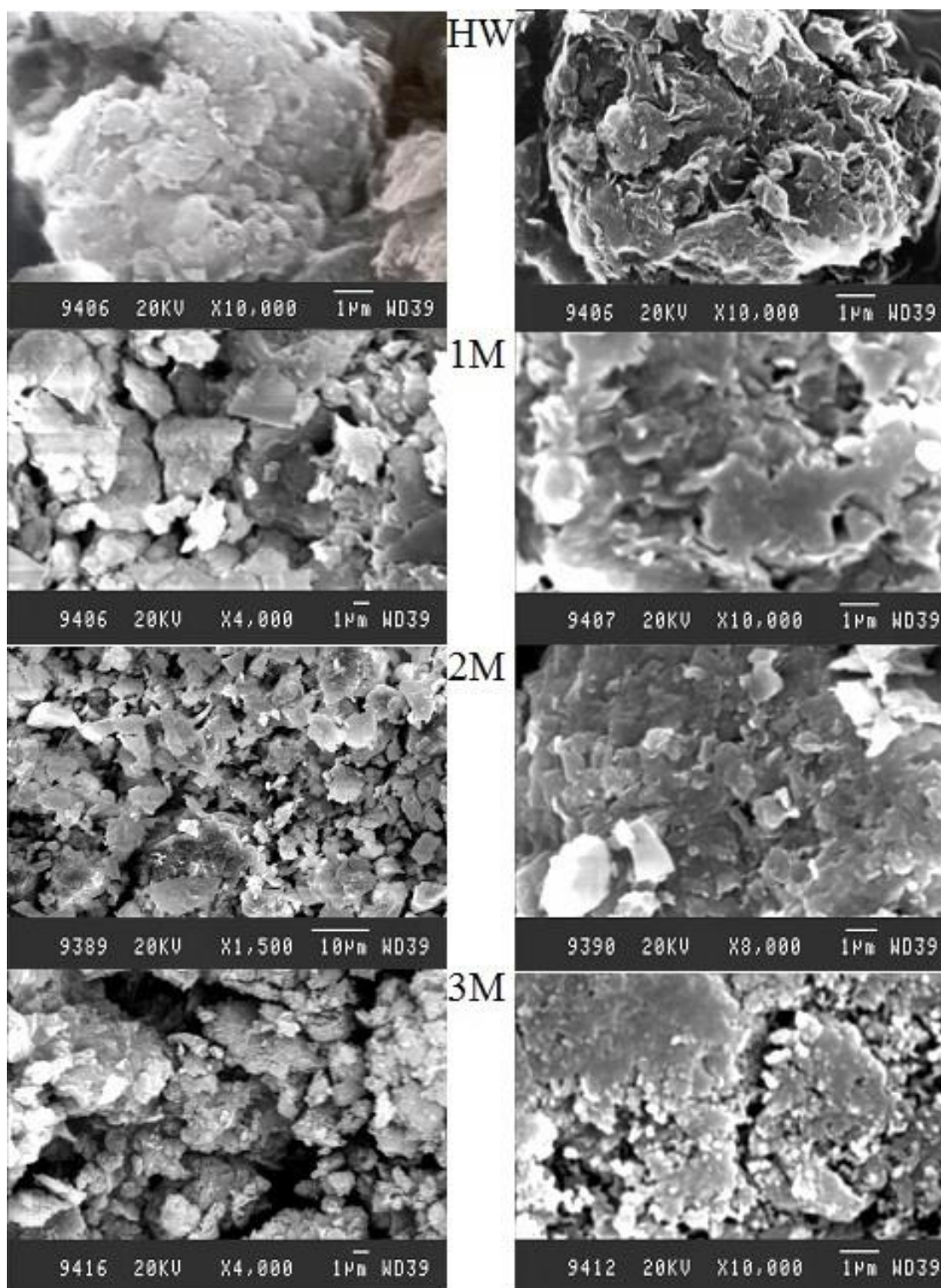


**Figure 1:** SEM images of HWB and acid activated samples.

The pore formation hypothesis by acid activation was also supported by the nitrogen sorption results (Figure 2 and Table 1). Crude bentonite reflected type II isotherm according to IUPAC classification with a very low gas adsorption value corresponding to micropore region ( $P/P_0 < 0.02$ ). While the

characteristic of the adsorption isotherm remained the same after acid activation, all activated samples showed H3 type hysteresis loop representative of the formation aggregates of plate particles or by porous solids, including cracks. As stated in the literature (17, 33) and supported by the chemical analysis (Table 1), at low acid concentration, the occurred octahedral alumina leaching increased the microporosity leading to the formation of pores in the octahedral sheet. As a result, a rise took place around 2.5 times in BET surface area value while the value of microporosity was doubled. The maximum BET surface area was achieved by activation with 2 M  $\text{H}_2\text{SO}_4$ , and micro pore volume attained to  $0.0340 \text{ cm}^3.\text{g}^{-1}$ . While these values remained nearly the same, a rise in mesopore volume took place from the partial silica decomposition with further concentration increase. The leaching from the tetrahedral sheet might result the formation of amorphous (free) silica with increased acid concentration, this could lead to a decrease of micro porosity and/or smooth channel constructions. The formation of macropores by acid strength was clearly seen in the isotherm. In this way the strength of pore wall weakens, the occurred pore wall breakage resulted increases in macroporosity by the formation of bigger size pores. The pore size distribution given in Figure 3 confirmed the apparent increase in micropore region with an average dimension of  $\sim 2 \text{ nm}$ . By the increase of acid concentration while micropores were exhibited a little lower size, the formation of mesopores in large quantities without uniform distribution was also observed.

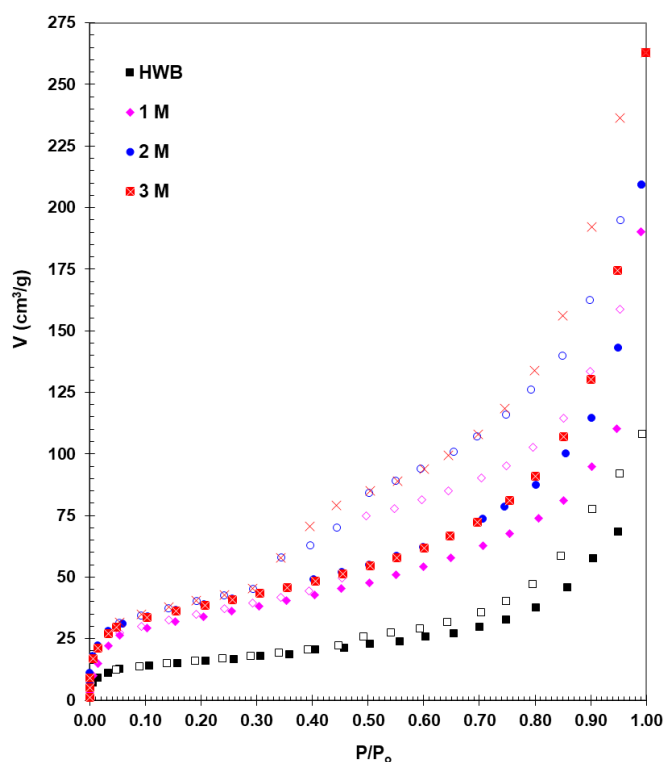


**Figure 2.** Nitrogen adsorption/desorption isotherms of HW and acid activated samples.

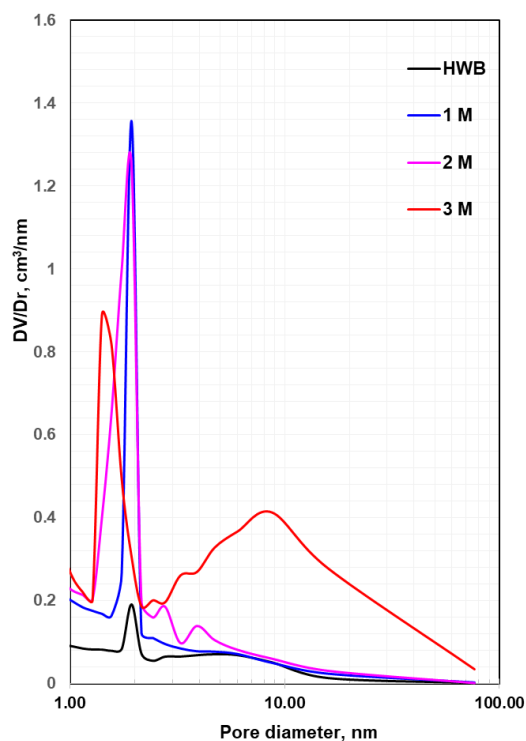


**Figure 3.** Pore-size distribution of HW and acid activated samples.

Removing impurities and dissolution of some oxides leaching as metal ions (mainly  $\text{Al}_2\text{O}_3$ , and octahedral metal ions such  $\text{Al}^{3+}$ ,  $\text{Fe}^{3+}$ ,  $\text{Fe}^{2+}$ , and  $\text{Mg}^{2+}$ ) were the source of the increase of surface area and left unsaturated valance bonds due to the removal of hydroxyl ions from the clay lattice. During the acid treatment, the replacement of exchangeable cations ( $\text{Ca}^{2+}$  and  $\text{Na}^+$ ) with  $\text{H}^+$  ions was the source of acidity increase (21). As expected, by metal leaching the formation of charged surfaces tripled the value of the surface acidity as measured by acid-base titration method (Table 1). While activation with 2 M  $\text{H}_2\text{SO}_4$  yielded a small increase, the rise-up of acid concentration to 3 M resulted over five-fold increase of surface acidity of crude bentonite.

We tried different surface groups to explain the phenomenon with FTIR spectra (Figure 4A). A series of vibration bands that are characteristic of smectite mineral were observed; the bands between 1200 and 400  $\text{cm}^{-1}$  wavenumbers as characteristics of silicate, corresponding to Si-O bonds in the tetrahedral sheet and the ones in the region of 1100–450  $\text{cm}^{-1}$  region characteristics of octahedral sheets were present in FTIR spectrum of as-mined bentonite. The 3000-3600  $\text{cm}^{-1}$  region represented the OH and water vibrations. The changes in FTIR bands by acid treatment were found in agreement with the literature (19, 21, 33-34).

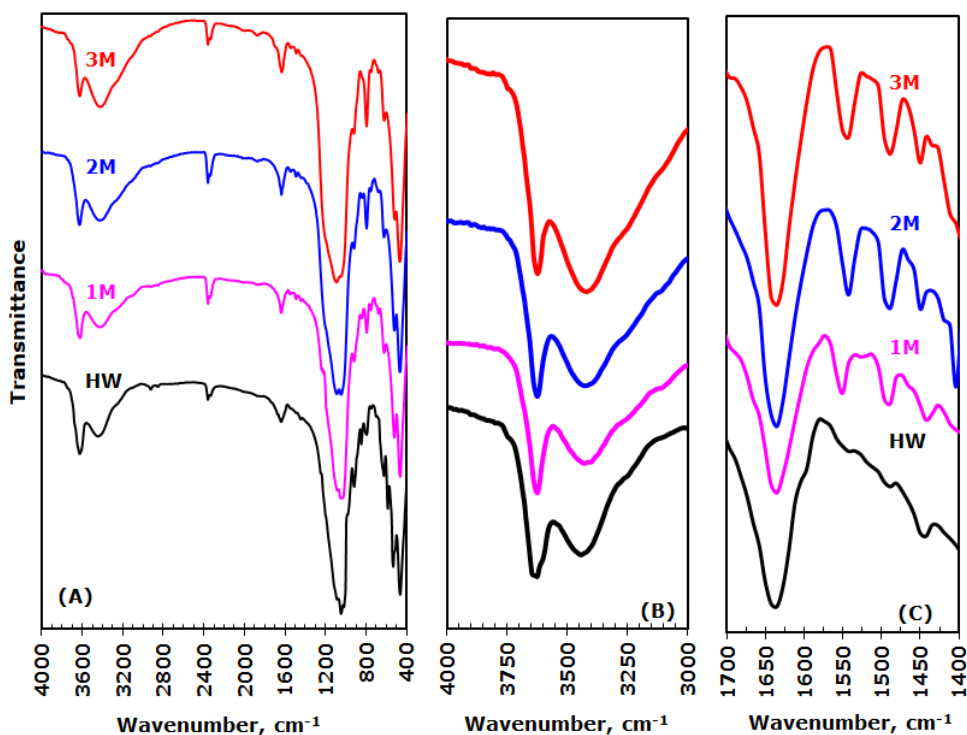


**Figure 4:** FTIR spectra of HWB and acid activated samples.

Bands at  $1050$  and  $532$   $\text{cm}^{-1}$ , corresponding to Si-O-Si stretching and Si-O deformation respectively, showed that the tetrahedral sheet of the clay was relatively stable and seemed that they were affected only at higher concentration. Although the wide band centered at  $1050$   $\text{cm}^{-1}$ , which was really composed of three separate ones with shoulders at  $1079$  and  $1025$  and  $980$   $\text{cm}^{-1}$ , were not affected much at low acid concentration, the structure became very sensitive to attacks of acid at higher concentrations and the variation in these bands become dominant by the increase of acid concentration. It is known that the formation of the amorphous silica with the increased acid concentration is inevitable. So the formation of free amorphous silica phase, and its quantity increase with a rise of acid concentration was evidenced by the prominence of the shoulders occurred at around  $1242$  and  $1095$   $\text{cm}^{-1}$  and the increase of the intensity peak was seen at around  $800$   $\text{cm}^{-1}$ . The other band ( $470$   $\text{cm}^{-1}$ ) was less sensitive than those. Dissolution of the octahedral sheets by acid activation was supported with FTIR spectra. The attack of acid to the octahedral metals caused decreases in the intensities of the peaks at  $920$ , and  $846$  ascribed to Al-Al-OH, and Al-Mg-OH, respectively. The final one was almost diminished with severe (3 M) acid treatment. The gradual intensity decreases with acid strength at  $627$   $\text{cm}^{-1}$  was caused by attacks of acid to either Al-OH or Si-O bending or Al-O stretching vibrations. The intensity of the band at  $467$   $\text{cm}^{-1}$  assigned to Si-O bending vibrations or Si-O-Al and Si-O-Mg coupled by OH vibrations stayed nearly as in the form of the crude bentonite. Vibrations ascribed to either Al-O-Si or Mg-O-Si and Al-Mg-OH at  $850$   $\text{cm}^{-1}$  decreased with increasing intensity. The dissolution of tetrahedral Si forming amorphous



silica resulted in increases in the peak intensity occurred at  $620\text{ cm}^{-1}$  which was also indicative of free silica formation. The bands appeared at  $790$  and  $470\text{ cm}^{-1}$  were also the characteristics of free silica and their intensities become dominant with the acid activation in parallel with the acid strength.

Si-O bending and Al-O stretching vibrations occurred at  $535\text{--}580\text{ cm}^{-1}$  which were decreased by acid activation. The band at  $448\text{ cm}^{-1}$  corresponds to Si-O bonding vibrational bonds in the smectites. The intensity of the band at  $460\text{ cm}^{-1}$  corresponds to Si-O bonding vibrational bonds in the smectites (Si-O-Al and Si-O-Mg coupled by OH vibrations or Si-O bending vibrations) was almost unchanged with increasing concentration of acid, although the shoulder caused by Al-O-Si vibration that appeared at  $524\text{ cm}^{-1}$  decreased at higher acid concentrations. A small increase in the intensity of water bending vibration caused by surface hydroxyl groups reflected a small band at  $1638\text{ cm}^{-1}$  and its intensity showed a weak rise with acid strength.

The stretching frequencies of the sharp peak at  $3628\text{ cm}^{-1}$  and the broad band at  $3450\text{ cm}^{-1}$  were attributed to the structural hydroxyl groups in the clay mineral layer and water molecules in the interlayer spaces. Although their locations were preserved, intensities of them showed great variation with the acid attack and acid concentration. AlAlOH coupled by AlMgOH stretching vibrations at  $3628\text{ cm}^{-1}$  decreases with increasing acid concentration. Evident increases occurred at the intensities of the former peak due to H bonding to OH, while the latter became more diffuse with the absorbed water. The band at  $3425\text{ cm}^{-1}$  resulted from water adsorbed on free silica and shoulder at  $3200\text{ cm}^{-1}$  assigned to the interlayer water became more diffuse with the increase of acid strength (Figure 3B).

The band at  $1444\text{ cm}^{-1}$  ascribed to the Lewis acid sites, the one at  $1487\text{ cm}^{-1}$  due to the contribution of Brønsted+Lewis acid site and two others at  $1542$  and  $1633\text{ cm}^{-1}$  belonging to Brønsted acid sites were vaguely in raw bentonite (Figure 4C) (35). All peaks representative of acid sites become more diffuse with increasing severity of treatment.

## CONCLUSIONS

The characterization results showed that the activation of bentonite with sulfuric acid leads to a significant improvement in structural and textural characteristics. The SEM photographs have shown that increases in acid concentration cause decreases in the particle sizes while it causes increases in pore dimensions and formation of new pores which were supported by nitrogen adsorption isotherms. Further increase of acid concentration (3 M) caused the pore wall deformation and led to the formation of bigger size pores, further increases resulted no noticeable change in the value. Considerable increases occurred both in surface acidity and surface area values until reaching 2 M acid concentration. By the metal leaching the formation of charges surfaces doubled the value of the surface acidity as measured by acid-base titration method. The FTIR spectra showed that octahedral sheets were attracted more than the tetrahedral sheets and severe acid treatment caused an increase in the OH deformation from the sheets and the formation of free silica was also observed. The increased silica/alumina ratio with partial delumination led to an increase in the number of weakly acidic Si-OH groups and subsequently to an increase in both Lewis and Brønsted acidities. Acid activation and structural properties close to those stated in the patents have been obtained by acid activation of Hangılı White Bentonite.

## ACKNOWLEDGMENT

This work is partially funded by Research Fund BAP 06/2009-20 of Gazi University. The author wishes to express her greatest thanks to Ayşen Dağeri for her help in the experimental study.

## REFERENCES

1. Velde, B. Introduction to clay minerals. Chapman Hall 1992; 42-61.
2. Velde B. Origin and mineralogy of clays: clays and the environment. Springer 1995 p.8.
3. Adams, J.M., McCabe, R.W. Clay minerals as catalyst in F. Bergaya, G. Lagaly (Eds.) Development in clay science: Handbook of clay science. 2013; vol. 5, 491–538.
4. Al-Zahrani, A.A., Al-Shahrani, S.S, Al-Tawil, Y.A. Study on the activation of Saudi natural bentonite, Part II: Characterization of the produced active clay and its test as an adsorbing agent. J. King Saud Univ., Eng. Sci. 2000; 13 (2): 193–203
5. Tjong, S.C. Synthesis and structure-property characteristics of clay-polymer nanocomposites in Tjong, S.C. (Ed.) Nanocrystalline materials. 2006; 311-348.
6. Nguyen, Q.T., Baird, D.G. Preparation of polymer–clay nanocomposites and their properties. Adv. Polym. Tech. 2006; 25 (4): 270-285.

7. Vicente, M.A., Gil, A., Bergaya, F. Pillared clays and clay minerals in F. Bergaya, G. Lagaly (Eds.) Development in clay science: Handbook of clay science 2013; vol. 5, 527-557.
8. Brezovska, S., Marina, B., Burevski, D., Angusheva, B., Boseska, V., Stojanovska, L. Adsorption properties and porous structure of sulfuric acid treated bentonites determined by the adsorption isotherm of benzene vapor. J. Serb. Chem. Soc. 2005; 70 (1): 33–40.
9. Zhansheng, W.U., Chun, L.I., Xifang, S., Xiaolin, X., Bin, D., Jine, L., Hongsheng, Z. Characterization, acid activation and bleaching performance of bentonite from Xinjiang. Chinese J. Chem. Eng. 2006; 14 (2): 253-258.
10. Noyan, H., Önal, M., Sarıkaya, Y. The effect of sulphuric acid activation on the crystallinity, surface area, porosity, surface acidity, and bleaching power of a bentonite. Food Chem. 2007; 105 (1): 156-163.
11. Önal, M., Sarıkaya, Y. Preparation and characterization of acid-activated bentonite powders. Powder Technol. 2007; 172 (1): 14-18.
12. Didi, M.A., Makhoukhi, B., Azzouz, A., Villemin, D. Colza oil bleaching through optimized acid activation of bentonite; A comparative study. Appl. Clay Sci. 2009; 42: 336–344.
13. Bieseki, L., Treichel, H., Araujo, A.S., Castellã Pergher, S.B. Porous materials obtained by acid treatment processing followed by pillaring of montmorillonite clays. Appl. Clay Sci. 2013; 85: 46-52.
14. Komadel, P., Madejová, J. Acid activation of clay minerals in F. Bergaya, G. Lagaly (Eds.) Development in clay science: Handbook of clay science. 2013; vol. 5, 385-409.
15. Al-Shahrani, S.S. Treatment of wastewater contaminated with cobalt using Saudi activated bentonite. Alexandria Eng. J. 2014; 53 (1): 205-211.
16. Bendou, S., Amrani, M. Effect of Hydrochloric Acid on the Structural of Sodic-Bentonite Clay. J. Miner. Mater. Charac. Eng. 2014; 2: 404-413.
17. Petrović, Z., Dugić, P. Aleksić, V., Begić, S., Sadadinović, J, Mičić, V., Kljajić, N. Composition, structure and textural characteristics of domestic acid activated bentonite. Contemp. Mater. 2014; 1: 133-139.
18. Madejová, J., Pálková, H., Jankovič, L. Near-infrared study of the interaction of pyridine with acid-treated montmorillonite. Vib. Spectrosc. 2015; 76: 22-30.
19. Komadel, P. Acid activated clays: Materials in continuous demand. Appl. Clay Sci. 2016; 131: 84-99.
20. Tayano, T., Uchino, H., Sagae, T., Ohta, S., Kitade, S., Satake, H., Murata, M. Locating the active sites of metallocene catalysts supported on acid-treated montmorillonite. J. Mol. Catal. A: Chem. 2016; 420: 228-236.
21. Akpomie, K.G., Dawodu, F.A. Acid-modified montmorillonite for sorption of heavy metals from automobile effluent. Beni-Suef University J. Basic and Appl. Sci. 2016; 5 (1): 1-12.
22. Makhoukhi, B., Didi, M. A., Villemin, D., Azzouz, A. Acid activation of bentonite for use as a vegetable oil bleaching agent. Grasas Aceites. 2009; 60 (4): 343-349.

23. Zhao, Y.H., Wang, Y.J., Hao, Q.Q., Liu, Z.T., Liu, Z.W. Effective activation of montmorillonite and its application for Fischer-Tropsch synthesis over ruthenium promoted cobalt. *Fuel Process Technol.* 2015; 136: 87-95.
24. Michelle J.C. Rezende, M.J.C., Pinto, A.C. Esterification of fatty acids using acid-activated Brazilian smectite natural clay as a catalyst. *Renew. Energ.* 2016; 92: 171-177.
25. Elfadly, A.M., Zeid, I.F., Yehia, F.Z., Abouelela, M.M., Rabie, A.M. Production of aromatic hydrocarbons from catalytic pyrolysis of lignin over acid-activated bentonite clay. *Fuel Process Technol.* 2017; 163: 1-7.
26. Yu, W., Wang, P., Zhou, C., Zhao, H., Tong, D., Zhang, H., Yang, H., Ji, S., Wang, H. Acid-activated and WOX-loaded montmorillonite catalysts and their catalytic behaviors in glycerol dehydration. *Chinese J. Catal.* 2017; 38(6): 1087-1100.
27. Taylor, D.R., Hills, W. Process for making acid activated bleaching earth using high susceptibility source clay and novel bleaching earth product. 1991; US-5008226.
28. Taylor, D.R., Jenkins, D.B., Acid activated clays. *Soc. Min. Eng. AIME Trans.* 1998; 282: 1901-10.
29. Taylor, D.R., Ungermann, C.B. Process for making acid activated bleaching earth using high susceptibility source clay and novel bleaching earth product. 1999. US- 5008226A.
30. Antonio Ortiz, N.J., Solis, S.G., Thomassiny, V.E., Ruf, F. Amorphous adsorbent, method of obtaining the same and its use in the bleaching of fats and/or oils. 2008 CA-2668729A1.
31. Balci, S., Gökçay, E. Effects of drying methods and calcination temperature on the physicochemical properties of iron intercalated clays. *Mater. Chem. Phys.* 2002; 76 (1): 46-51.
32. Yu, K., Kumar, N., Aho, A., Roine, J., Heinmaa, I., Murzin, D.Y., Ivaska, A. Determination of acid sites in porous aluminosilicate solid catalysts for aqueous phase reactions using potentiometric titration method. *J. Catal.* 2016; 335: 117-124
33. Yıldız, N., Aktaş, Z., Çalimli, A. Sulphuric acid activation of a calcium bentonite. *Particul. Sci. Technol.* 2004; 22 (1): 21-33.
34. Christidis, G. E., Scott, P.W., Dunham, A.C. Acid activation and bleaching capacity of bentonites from the islands of Milos and Chios, Aegean, Greece. *Appl. Clay Sci.* 1997; 12 (4): 329-347.
35. Auer, H., Hofmann, H. Pillared clays characterization of acidity and catalytic properties and comparison with some zeolites. *Appl. Catal. A-Gen.* 1993; 97 (1): 23-38.